



## IBIC analysis of high-power devices

T. Osipowicz<sup>a,\*</sup>, M. Zmeck<sup>a</sup>, F. Watt<sup>a</sup>, G. Fiege<sup>b</sup>, L. Balk<sup>b</sup>, F. Niedernostheide<sup>c</sup>,  
H.-J. Schulze<sup>c</sup>

<sup>a</sup> *Physics Department, Research Centre for Nuclear Microscopy, National University of Singapore, Lower Kent Ridge, Singapore 119260, Singapore*

<sup>b</sup> *Universität Wuppertal, Fachbereich Elektrotechnik, Lehrstuhl für Elektronik, Fuhlrottstr.10, D-42097 Wuppertal, Germany*

<sup>c</sup> *Siemens AG, Corporate Technology, Otto-Hahn-Ring 6, D-81730 Munich, Germany*

---

### Abstract

The technique of ion beam induced charge microscopy (IBIC microscopy) has been used for several years to analyse integrated circuits, radiation detectors and solar cells [H. Schöne, D.N. Jamieson, MRS Bull. 25 (2000) 14]. In this work, results from a first attempt to investigate high-power devices with this technique are reported. It is demonstrated that IBIC analysis allows the characterisation of layers of different doping types located several tens of microns below the sample surface with an ion beam energy of 2 MeV. The devices investigated are high-power light-triggered thyristors [M. Ruff, H.-J. Schulze, U. Kellner, IEEE (ED) 46 (1999) 1768; F.-J. Niedernostheide, H.-J. Schulze, J. Dorn, U. Kellner-Werdehausen, D. Westerholt, in: Proceedings of the 12th International Symposium on Power Semiconductors and IC's, ISPSD'2000, Toulouse, France, 2000, p. 267]. © 2001 Elsevier Science B.V. All rights reserved.

*Keywords:* IBIC; High-power device

---

### 1. Introduction

The techniques of electron beam-induced current microscopy (EBIC microscopy) and IBIC microscopy are complementary tools for the analysis of microelectronic devices [1,4]. An electron beam of 40 keV energy has a penetration depth of about 10  $\mu\text{m}$  in silicon, but the large lateral spread of the beam limits the resolution of EBIC for buried structures and geometries that involve layer structures which are tens of microns

thick. IBIC microscopy, on the other hand, carried out with a proton beam of 2 MeV, has a penetration depth of 47  $\mu\text{m}$  in Si with only a few microns lateral spread of the beam. This large penetration depth allows buried active junctions to be analysed with reasonable lateral resolution. Therefore, IBIC microscopy seems well suited for the analysis of high-power devices. High-power thyristors, for example, require p–n junctions located about 100  $\mu\text{m}$  below the surface to achieve sufficiently high breakdown voltages of the order of 10 kV. In this paper, we report on the first results from the IBIC analysis of high-power light-triggered thyristors. A very uniform doping level of the n<sup>-</sup> base and a uniform depth of the diffused

---

\* Corresponding author. Tel.: +65-772-6745; fax: +65-777-6126.

E-mail address: phyto@leonis.nus.edu.sg (T. Osipowicz).

p layer are required in these elements to prevent local excessive fields, which could initiate breakdown inside the semiconductor structure. The eventual aim of the work is to determine whether IBIC images can be correlated with device performance, but in this paper we will only demonstrate that IBIC imaging of high-power thyristors [2,3] is possible. The ion beam creates considerable damage to the lattice structure of the device. Therefore, it is necessary to quantify damage generation as well.

## 2. Experimental setup

The measurements were carried out at the National University of Singapore Nuclear Microscopy facility [5]. A sketch of the experimental setup used for the IBIC measurements is shown in Fig. 1. The ion beam from the Van de Graaff accelerator is focused to produce a beam spot of around  $1\ \mu\text{m}$  size, and the collimators are adjusted to produce a beam intensity up to  $\sim 1000$  ions/s. Different regions of the thyristor device were contacted either directly by tungsten needles or simply by contacting the cathode and anode of the main thyristor. All measurements reported here were carried out without external biasing of the devices. The IBIC signals are fed to an Oxford Microbeams data acquisition system via a charge sensitive preamplifier (ORTEC 142a). Calibration of the pulse height spectra is achieved by the accumulation of an RBS spectrum of a calibrated sample with the same electronic setup. List-mode

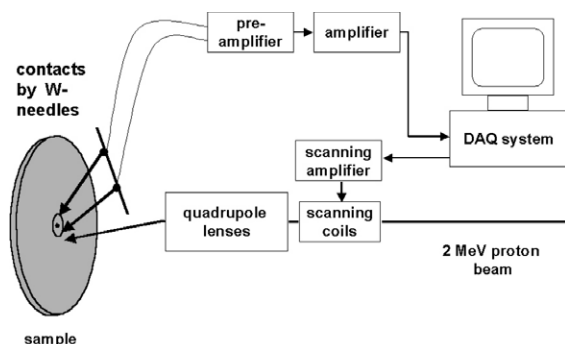


Fig. 1. Experimental setup used for IBIC microscopy.

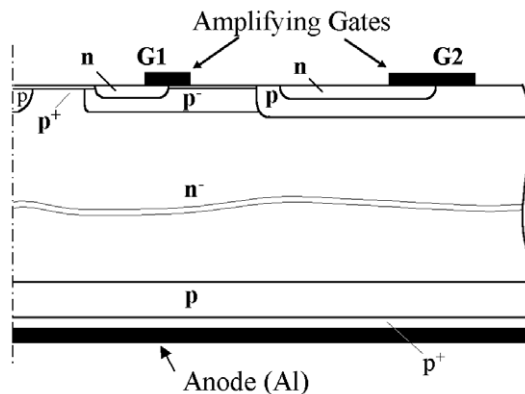


Fig. 2. Cross-section of one half of the centre region of the axially symmetric light-triggered thyristor.

data acquisition is used, allowing for off-line data analysis. Because good contrast is found in off-line generated images that represent the mean value of the charge collection spectrum at each pixel, the images presented here were generated in this way. A proton beam with 2 MeV energy was used in the measurements.

The structure of the investigated thyristor is shown in Fig. 2. In all experiments the sample was mounted so that the ions penetrated into the thyristor from its upper side (cathode side).

## 3. Results

Fig. 3 shows an IBIC image of the centre of a light-triggered thyristor. The ion dose used was  $1.1\ \text{p}/\mu\text{m}^2$ . For this measurement the central p region, being part of the light-sensitive central p–n<sup>−</sup> junction, and the cathode contact of the first amplifying gate (G1 in Fig. 2) were connected to the preamplifier. The three depletion regions vertical to the surface are all producing contrast. The inner two p–n<sup>−</sup> junctions are buried by the  $10\ \mu\text{m}$  thick p<sup>+</sup> layer, and these junctions provide the highest contrast. This contrast is generated by induced charges collected in the space charge. Electron/hole pairs are generated at a roughly constant rate along the ion beam path, with a peak close to the end of range. Due to the relatively large diffusion length in the n<sup>−</sup> region a large part of the gener-

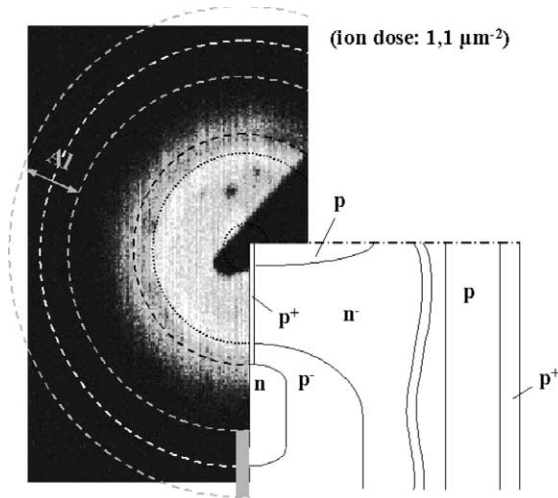


Fig. 3. IBIC image and schematic diagram of an unprepared thyristor; the central p region and the inner metal ring were connected to the preamplifier.

ated charge carriers reach either one of the vertical p–n<sup>-</sup> junctions.

Fig. 4 shows an IBIC image of the same device, with the anode and cathode contacts of the main

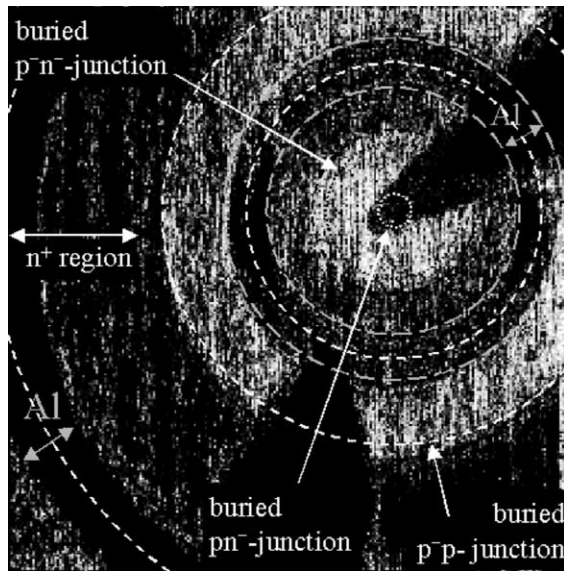


Fig. 4. IBIC image of an unprepared thyristor; anode and cathode of the main thyristor were connected to the preamplifier.

thyristor connected to the preamplifier. The two W-needles, which are connected to the central p region and the first amplifying gate (G1), were not removed. In this configuration the depletion region of the p<sup>-</sup>–n<sup>-</sup> junction at a depth of about 100 μm is used as the collecting junction. Despite the very small ion dose of about 0.06 μm<sup>-2</sup> and the fact that the ion penetration depth of 47 μm is appreciably smaller than the depth of the active p<sup>-</sup>–n<sup>-</sup> junction, several layers of the thyristor can be identified in the image: the strongest signal is observed in the n<sup>-</sup> region in the centre of the device, where the low doping level produces the largest diffusion length and the largest extent of the space charge region. The higher doping of the p region results in a smaller diffusion length so that less charge collection occurs. The n emitter regions of the first and second amplifying gates do not appear in the image because they are shorted with the surrounding p layers by metal rings [6]. Furthermore, the metal rings cause a reduction in the energy of the ions resulting in a reduced signal intensity in the region below the Al-metallisation.

Fig. 5 shows an IBIC image of the central thyristor region, taken from a sample where all

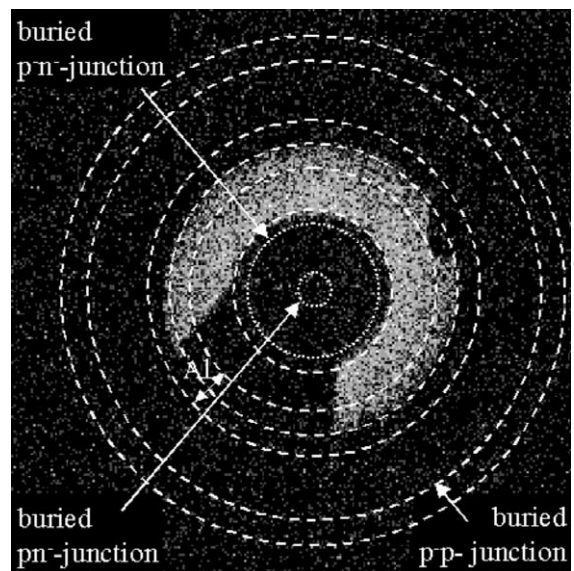


Fig. 5. IBIC image of a thyristor without any metal layers; the central p region and the n emitter region of G1 (Fig. 1) were connected to the preamplifier.

metal layers were removed. The preamplifier was connected to the central p region and the  $n^+$  emitter of the first amplifying gate. Due to the removal of the amplifying gate metallisation the shorts between the  $n^+$  emitter and the  $p^-$  base do not exist anymore, leading to images different from Fig. 3: the directly connected n region produces a high signal but no other structures are visible.

In Fig. 6 an IBIC image of a thyristor sample is shown after all metal layers and several tens of  $\mu\text{m}$  of the Si surface were etched off from the cathode-side surface. The ion dose was about  $0.25 \text{ p}/\mu\text{m}^{-2}$ . The preamplifier was connected to the central p region of the device and the  $p^-$  region. In the image a high contrast in the central region of the device, with the highest signal and the two inner vertical  $p-n^-$  junctions, can be seen. Although the  $p^+$  layer and, therefore, the lateral  $p^+-n^-$  junction close to the centre of the thyristor was removed, there is still IBIC intensity generated in this region. This result provides further evidence for the assumption that the contrast in this region is mainly produced by the diffusion of the generated charge carriers to the vertical  $p-n^-$  junctions. Note that

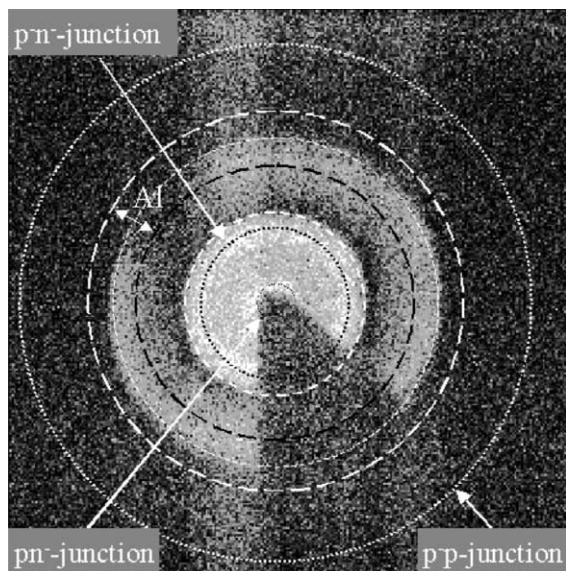


Fig. 6. IBIC image of a thyristor with several tens of  $\mu\text{m}$  etched from the surface; the central p region and the  $p^-$  region were connected to the preamplifier.

the distance between the deep lateral  $p^-n^-$  junction and the surface is reduced for this sample. Even though the  $n^-$  region is not connected to the preamplifier, it still produces contrast in the image. Such “unconnected junction contrast”, assumed to be generated by transient currents due to parasitic capacitances, has been reported earlier [5].

#### 4. Conclusions and outlook

In spite of the large dimensions of high-power devices, buried layers can be analysed by means of the IBIC microscopy. Because rather small ion doses are sufficient to generate well-resolved IBIC images, non-destructive analysis of the devices is possible. The 3.5 MeV HVEE Singletron accelerator recently commissioned and installed at the Research Centre for Nuclear Microscopy, Singapore will be used for IBIC measurements on similar devices with an ion beam energy of 3.5 MeV, because the longer range of ions will allow the deeply buried junctions to be imaged with better sensitivity: the penetration depth of 3.5 MeV protons is in the range of 100  $\mu\text{m}$ , comparable to the depth of the lateral  $p^-n^-$  junction used as collecting junction region in the configuration with anode and cathode of the main thyristor connected to the preamplifier. Furthermore, cooling of the device will be implemented to increase the signal-to-noise ratio of the IBIC signal.

#### References

- [1] H. Schöne, D.N. Jamieson, MRS Bull. 25 (2000) 14.
- [2] M. Ruff, H.-J. Schulze, U. Kellner, IEEE (ED) 46 (8) (1999) 1768.
- [3] F.-J. Niedernostheide, H.-J. Schulze, J. Dorn, U. Kellner-Werdehausen, D. Westerholt, in: Proceedings of the 12th International Symposium on Power Semiconductors and IC's, ISPSD'2000, Toulouse, France, 2000, p. 267.
- [4] M.B.H. Breese, D.N. Jamieson, P.J.C. King, Materials Analyses Using a Nuclear Microprobe, Wiley, New York, 1996.
- [5] F. Watt, I. Orlic, K.K. Loh, C.H. Sow, P. Thong, S.C. Liew, T. Osipowicz, T.F. Choo, S.M. Tang, Nucl. Instr. and Meth. B 85 (1994) 708.
- [6] T. Osipowicz, J.L. Sanchez, I. Orlic, F. Watt, S. Kolachina, V.K.S. Ong, D.S.H. Chan, J.C.H. Phang, Nucl. Instr. and Meth. B 130 (1997) 503.